Acta metall. mater. Vol. 39, No. 4, pp. 627–639, 1991
Printed in Great Britain.

0956-7151/91 $3.00 + 0.00

PENETRATION OF TIN AND ZINC ALONG TILT GRAIN BOUNDARIES 43° [100] IN Fe–5 at.% Si ALLOY: PREMELTING PHASE TRANSITION?

E. I. RABKIN, V. N. SEMENOV, L. S. SHVINDLERMAN and B. B. STRAUMAL

Institute for Solid State Physics, Academy of Sciences of the U.S.S.R., Chernogolovka, Moscow District, 142432 U.S.S.R.

(Received 13 September 1989; in revised form 24 July 1990)

Abstract—Tin and zinc penetration along the tilt grain boundary 43° [100] in b.c.c. Fe–5 at.% Si alloy is studied in the temperature range from 652 to 975°C. Wetting transition of grain boundary by the tin-rich melt at $T_w = 810 \pm 5$°C is observed. Above T_w there is a thin wetting film at grain boundary. With zinc penetration along the grain boundary a wetting film has been observed at all temperatures studied. Behind that film there is a region with an unusually high diffusivity of zinc, and below that region there is a region of "ordinary" grain boundary diffusivity. Such a phenomenon may be explained in terms of the phase transition "grain boundary–thin wetting film on the boundary", which is commonly known as a premelting phase transition. A model is proposed which explains the form of the temperature dependence of the concentration c_{Bt}, at which such transition occurs, and, in particular, the influence of the "paramagnet–ferromagnet" transition in the bulk on the premelting transition. The influence of the temperature dependence of the volume solubility limit, c_0, on the $c_{Bt}(T)$ dependence is also discussed. In critical region below Curie point T_c critical exponents d of magnetic part of activation free energy of bulk and grain boundary diffusion are calculated. Critical index d for grain boundary diffusion by premelting layer, as well as activation energy in paramagnetic region, lies in the interval between bulk values of d and estimation of d for truly two-dimensional grain boundary diffusion.

Résumé—On étudie la pénétration de l'étain et du zinc dans le joint de grains de flexion 43° [100] dans l'alliage cc Fe–5 at.% Si dans la gamme de températures de 652 à 975°C. A $T_w = 810 \pm 5$°C. On observe une transition de mouillage du joint de grains par la phase fondue riche en étain. Au dessus de T_w, apparait un film mince mouillant suivant le joint de grains. Avec la pénétration du zinc dans le joint de grains, on observe un film mouillant dans tout l'intervalle de température étudié. Derrière ce film, il existe une région aù la diffusion du zinc est anormalement rapide, et au dessous de cette région, une autre où la diffusion intergranulaire est "normale". On peut expliquer ce phénomène en se référant à une transformation de phases "joint de grains–film mince mouillant au joint", connue habituellement sous le nom de préfusion. On propose un modèle qui explique le mode de dépendance de la concentration c_{Bt}, à laquelle se produit cette transformation, en fonction de la température et qui explique, en particulier, l'influence de la transition "para-ferromagnétique" en volume sur la transformation de préfusion. L'influence de la dépendance, en fonction de la température, de la limite de solubilité en volume c_0 sur la fonction $c_{Bt}(T)$ est discutée. Dans le domaine critique, au dessous du point de Curie T_c, on calcule les exposants critiques d de la partie magnétique de l'énergie libre d'activation de la diffusion en volume et de la diffusion intergranulaire. L'indice critique d pour la diffusion intergranulaire sur une couche préfondue se trouve compris entre les valeurs de d en volume et l'estimation de d pour une diffusion intergranulaire vraiment bidimensionelle.

Zusammenfassung—Das Eidringen von Zinn und Zink an der [100]- 43°-Kippkorngrenze in der krz Legierung Fe–5 At. – % Si wurde im Temperaturbereich von 652 bis 975°C untersucht. Ein Phasenübergang der Benetzung der Korngrenze durch die Zinnreiche Schmelze wird bei $T_w = 810 \pm 5$°C beobachtet. Oberhalb von T_w liegt ein dünner benetzender Film an der Korngrenze. Bei Durchdringungsversuchen mit Zink war die benetzende Schicht im gesamten Temperaturbereich vorhanden. Unterhalb dieses Filmes findet sich eine Zone ungewöhnlich hoher Zink-Diffusion, und darunter eine Zone "normaler" Korngrenzdiffusion. Eine solche Erscheinung kann mit einem Phasenübergang "Korngrenze–dünner benetzender Film an der Korngrenze" beschrieben werden, der als Phasenübergang des Vorschmelzens bekannt ist. Es wird ein Modell vorgeschlagen, welches die Form der Temperaturabhängigkeit der Konzentration c_{Bt}, bei der ein solcher Übergang auftritt, und insbesondere den Einfluß des Überganges "Paramagnet–Ferromagnet" im Volumen auf den Vorschmelz-Übergang erklärt. Der Einfluß der Temperaturabhängigkeit der Volumlöslichkeitsgrenze c_0 auf die c_{Bt}-Abhängigkeit wird ebenso diskutiert. Im kritischen Bereich unterhalb des Curie-Punktes T_0 wurden die kritischen exponenten des magnetischen Teiles der freien Aktivierungsenergie für Volum- und Korngrenzdiffusion berechnet. Der kritische Exponent d für Korngrenzdiffusion durch die Vorschmelzschicht, wie auch die Aktivierungsenergie im paramagnetischen Zustand, liegt zwischen dem Volumwert von d und der Abschätzung von d für echte zweidimensionale Korngrenzdiffusion.

1. INTRODUCTION

Phase transitions in two-dimensional systems have attracted physicists' attention in recent years. According to the transmission microscopy data, the grain boundary thickness makes up 2 or 3 lattice parameters [1]. This is roughly the same as the thickness of distorted layer on surface of solids [2]. So it is no by chance that grain boundaries and surfaces have similar features. In particular, the results of computer simulation of grain boundaries structure [3–8], the electron microscopy data [9, 10], and the investigations of grain boundary migration, surface tension and diffusion [11–14] indicate that phase transitions on surface and on grain boundaries have much in common. In particular, the phase transitions accompanying wetting of interfaces in solids [15, 16], are very interesting. At such transitions (prewetting, premelting) a thin equilibrium layer of another phase, which is unstable in the sample's bulk, is formed at the interface. Wetting of grain boundaries by the melt in two-component systems is commonly known phenomenon and was actually observed in a lot of systems (Zn–Sn [17, 18], Al–Sn [19–21], Al–Pb [19], Ag–Pb [22]). Below the wetting temperature T_w, the contact angle at the intersection of grain boundary and the interface "melt–solid" is constant and roughly equals 180°. When $T \Rightarrow T_w$ this angle decreases fastly, and at $T > T_w$ a melt layer appears on grain boundaries.

On the other hand, the theoretically predicted [23–27] phase transitions accompanied by formation of thin liquid layers on boundaries (premelting, prewetting) has never been observed experimentally in solids. This may be explained in the following way. In systems, for which the wetting of grain boundaries by the melt was observed (Zn–Sn [17, 18], Al–Sn [19–21], Al–Pb [19], Ag–Pb [22]) the region of existence of solid solution based on the component with higher melting temperature is very narrow. The features of prewetting were only observed in Ref. [14], where the anomalous behavior of diffusion by grain boundaries and interphase boundaries was explained from the viewpoint of Cahn's transitions.

In this study we have tried to find and investigate the wetting and premelting transitions in systems with high enthalpy of mixing Fe–Sn and Fe–Zn [28]. In system Fe–Sn there exists a critical point of immiscibility in melt [29], and in system Fe–Zn the line of solubility limit in the solid solution based on the b.c.c.-iron is placed very near to the metastable curve of solid solution decomposition, and the "virtual" critical point of this curve lies only a little above the peritectic temperature [29, 30]. According to Ref. [31] such systems are appropriate candidates for the grain boundary wetting. On the other hand, the region of existence of Fe-based solid solution in those systems is large enough for the registration of changes in grain boundaries properties at the prewetting or premelting transition. In order to study such changes in grain boundary kinetic properties we have measured parameters of grain boundary and bulk interdiffusion of Sn or Zn and Fe. We have not only defined the activation energy and the diffusion pre-exponential factor values, but we have also tried to analyze the diffusion coefficients behaviour in the critical region below the temperature of magnetic transition T_c using the so-called critical indices, widely used in the theory of phase transitions.

2. EXPERIMENTAL

All experiments were carried out on the bicrystals of alloy Fe–5 at.% Si. This is the minimum percentage of silicon which is enough to isolate the region of existence of γ-phase on binary diagram Fe–Si and thus makes it possible to grow single crystals and bicrystals with b.c.c.-lattice [29]. Alloy Fe–5 at.% Si was prepared using the armco–iron and the silicon of semiconducting purity. The specimens were grown by electron-beam zone melting in vacuum of 10^{-6} torr. Growth rate was 1 mm per min. A bicrystal with a general tilt boundary [100] and misorientation angle 43° was grown. The misorientation angle was determined by etch pits and by optical orienting with laser light source. The accuracy of angle measurements made up $\pm 0.5°$. The as-grown bicrystal 12 mm in diameter was cut by electro-spark cutter into specimens of length 6 . . . 12 mm and of cross-section of $1.5 \times 1.5\ mm^2$. The boundary lay in the middle, and was orthogonal to the longer side of the specimen. A layer of tin or zinc was applied to each of the specimens by immersion into melt. Before immersion the specimens were ground mechanically and afterwards chemically polished in a solution of 80% H_2O_2 + 14% H_2O + 6% HF. Then the applied layer was completely removed from the two lateral faces of the specimen, and from two faces the excess zinc or tin was removed and only a layer of 100 . . . 150 μm thickness was left.

The samples were sealed into evacuated quartz ampoules. Then they were annealed in a furnace in the temperature range between 660 and 908°C. Anneals temperatures and durations are displayed in Table 1. After annealing, the samples were fixed in a holder using the Wood alloy, then mechanically ground and polished surface of specimens was etched for 10 . . . 15 s in order to visualize the grain boundary and to prepare specimens for an optical microscope study. The site of grain boundary intersection with the specimen surface was marked by imprints of indentor of an installation for microhardness determination. Then the sample was re-polished mechanically: the relief created by chemical etching was removed, while the indentations remained. Then the tin or zinc distributions were measured by means of electron-beam microprobe analysis [cf. Fig. 1(a)]. In order to calculate concentration from intensities of characteristic X-ray radiation, the corrections were introduced using standard methods of qualitative

Table 1. The tin bulk diffusion coefficients for Fe–5 at.% Si alloy

Temperature (°C)	Anneal duration, $t \times 10^{-4}$ s.	Diffusion coefficient, $D_{Sn} \times 10^{17}$ m^2/s
908	1.08	4200
862	4.32	1900
838	24.48	1300
813	19.44	660
792	18.00	460
772	39.60	250
753	36.00	180
745	60.12	74
740	28.08	110
737	48.60	59
734	43.20	72
728	30.60	52
725	28.80	38
721	34.56	36
719	49.32	30
719	61.20	23
717	43.56	21
714	76.50	28
711	83.52	24
706	79.20	15
702	68.40	9.5
692	77.76	8.5
685	90.18	5.4
667	101.5	4.7
652	293.8	1.6

X-ray spectra analysis [32]. The silicon concentration checks showed that the concentration oscillated stochastically in range 5 ± 0.2 at.%. Therefore, we assumed the silicon concentration constant and used the diffusional equations for a two-component system.

The tin bulk diffusion coefficient D was determined by equation

$$c(y, t) = c_0 [1 - \mathrm{erf}(y/2\sqrt{Dt})]$$

which is the solution of diffusional equation with boundary conditions $c(0, t) = c_0$ and $c(\infty, t) = 0$ [33]. Here y is the distance, t-time, erf-error function. Practically, in order to define D, dependences of $4t/y^2$ upon $[\mathrm{erf}^{-1}(1 - c/c_0)]^{-2}$ were plotted. If D does not depend on concentration, then these dependences must be straight lines, incident with the origin, the tangent of angle between them and x-axis being equal to D. Precisely this picture can be seen in Fig. 2(a, b), where dependences of $4t/y^2$ upon $[\mathrm{erf}^{-1}(1 - c/c_0)]^{-2}$ for tin diffusion at two different temperatures are plotted.

For zinc diffusion, the straight line drawn through experimental points in coordinates $4t/y^2$ upon $[\mathrm{erf}^{-1}(1 - c/c_0)]^{-2}$ are not incident to the origin [Fig. 2(c, d)]. This is explained by the fact that in iron–silicon alloy the zinc diffusion coefficient depends strongly on zinc concentration. We shall take this dependence into account by Lyubov's method

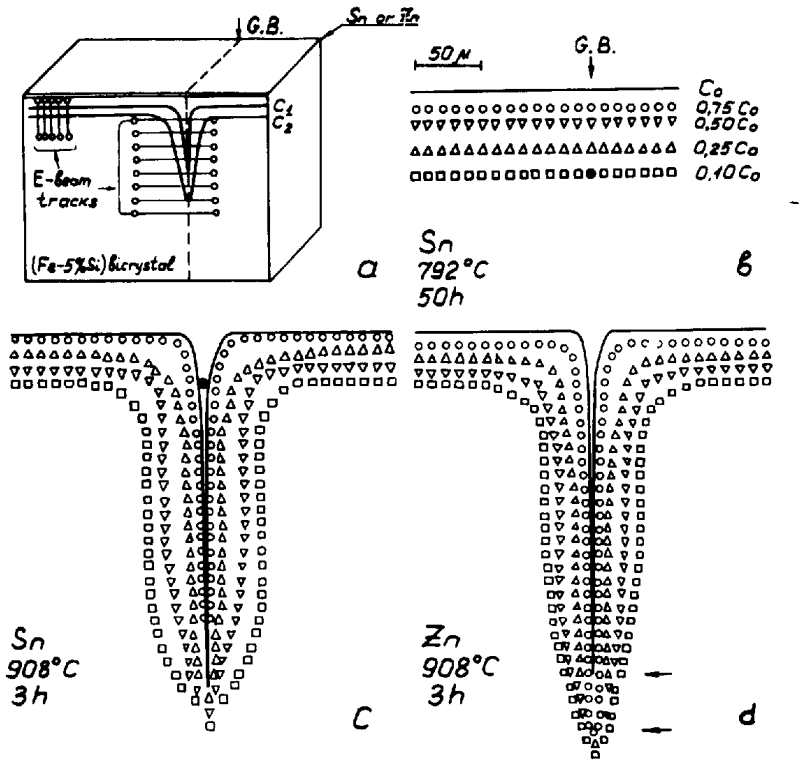

Fig. 1. (a) The scheme of concentration measurement in bicrystal after diffusional anneal. The isoconcentration lines and the plot of electron probe shift are drawn. The measurements were carried out in local X-ray spectrum analysis technique. (b) The distribution of tin concentration in a bicrystal with tilt boundary 43° [100] in alloy Fe 5 at.% Si after anneal at 792°C for 50 h. Five isoconcentration profiles are displayed. c_0 is the tin solubility limit. (c) The same as in Fig. 1(b) 908°C, 3 h. The black dot on the grain boundary is at such a distance from the sample surface, at which away from the boundary (in the bulk diffusion layer) the concentration of zinc equals $0.1c_0$ (cf. also b). (d) The zinc concentration in the same bicrystal after anneal at 908° for 3 h. The region of rapid grain boundary diffusion below the wetting layer is marked by arrows.

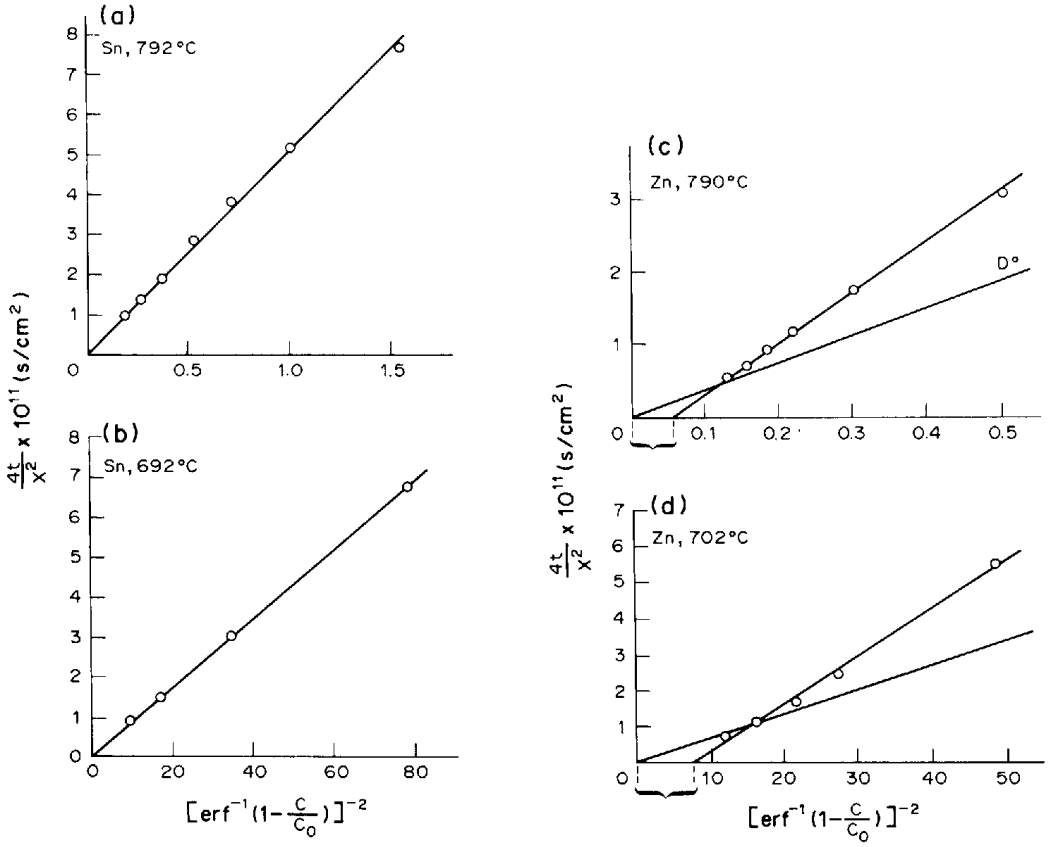

Fig. 2. Bulk diffusion profiles of zinc and tin for different temperatures plotted in coordinates $(4t/y^2)$ vs $[\mathrm{erf}^{-1}(1-c/c_0)]^2$. The tin diffusion coefficient does not depend on concentration, while that of zinc does. The D° value was determined by Lyubov's method [34]: A—tin diffusion, 792°C, 50 h; B—tin diffusion, 692°C, 216 h; C—zinc diffusion, 702°C, 190 h; D—zinc diffusion, 790°C, 63 h.

[34] assuming the diffusion coefficient to depend linearly upon the concentration c

$$D = D^0(1 + \beta c).$$

Here, β and D^0 are parameters. Assuming β to be small we may obtain the diffusion equation solution in the first order of the perturbation theory

$$\begin{aligned} c(y,t) = c_0[1 - \mathrm{erf}(\xi/2)] + (\beta c_0^2/2\sqrt{\pi})\xi \\ \times \exp(-\xi^2/4)[1 - \mathrm{erf}(\xi/2)] \\ + (\beta c_0^2/2)\mathrm{erf}(\xi/2)[1 - \mathrm{erf}(\xi/2)] \\ + (\beta c_0^2/\pi)[1 - \mathrm{erf}(\xi/2) - \exp(\xi^2/2)], \quad (1) \end{aligned}$$

where $\xi = y/\sqrt{D^0 t}$.

It is shown in the monography [35] that this solution is a good approximation if D does not change more than by a factor of 2. We defined the parameters D^0 and β values obtaining by computer calculations the best agreement between experimental and calculated curves $c(y, t)$. By this procedure, from 5 to 7 diffusion profiles measured at distance no less than $\sqrt{Dt}$ from each other were processed and averaged.

For definition of grain-boundary zinc diffusion coefficient, the diffusion profiles were measured along lines, perpendicular to grain boundary [parallel to sample surface to which diffusant was applied, cf. Fig. 1(B)] spaced form each other by 5 ... 10 μm. Such concentration profiles had the outlook of curves with the maximum c_B on grain boundary. The product of grain boundary diffusion coefficient D' and diffusional grain-boundary thickness δ was defined by Fisher's method. The usual equation for $D'\delta$ has the form

$$D'\delta = 2y^2\sqrt{D/\pi t}/[\log(c_B/c_0)]^2. \quad (2)$$

Here y is the distance along grain boundary [cf. Fig. 1(b)]. In Fig. 3 the dependences of grain boundary zinc concentration c_B upon depth y for various

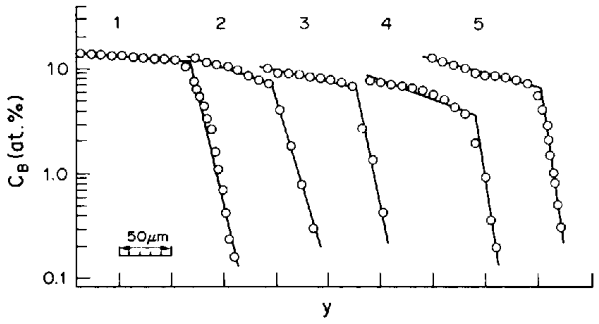

Fig. 3. The dependences of zinc concentration on boundaries c_B on depth y for different temperatures. At concentration c_{Bt}, the value of product of diffusion coefficient and boundary width $D'\delta$ is changed abruptly. The product is measured by the slope of $c_B(y)$ dependences. The c_{Bt} concentration is changed with temperature. (1) 975°C, 1.75 h; (2) 857°C, 7.5 h; (3) 809°C, 21 h; (4) 790°C, 63 h; (5) 745°C, 102 h.

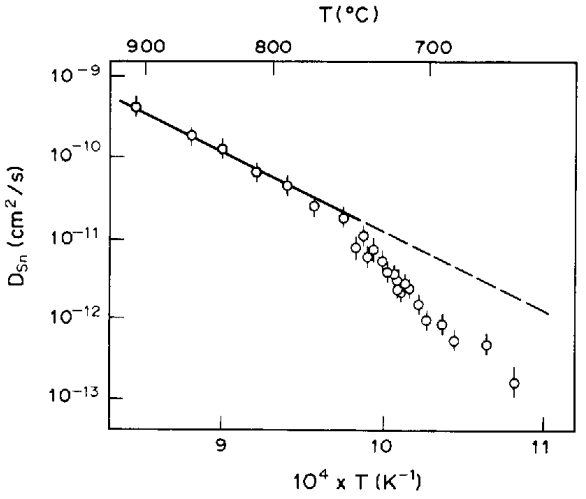

Fig. 4. Temperature dependence of the tin bulk diffusion coefficient in alloy Fe–5 at% Si along [100] direction.

temperatures are plotted in Fisher's coordinates. Each dependence has two regions: gentle for concentrations c_B near to bulk solubility limit c_0 and steep for concentrations below some concentration c_{Bt}. The reasons for such unusual behavior will be discussed below.

To determine the product $D'\delta$ by equation (2) using the Fisher's formula as an asymptotic form of the Whipple's equation [36], it is obligatory that Le Clair's condition [37] is observed

$$\beta_{lc} = D'\delta/(D\sqrt{Dt}) \gg 1. \quad (3)$$

We should note in advance that in our work the β_{lc} value for diffusion at c_B values higher than c_{Bt} (gentle region in Fig. 3) varies from 14.7 down to 10.1 in the temperature interval 908 . . . 652°C. Consequently, the equation (2) is of no doubt valid.

We have taken into account (within the framework of Fisher's model) the effect of concentration dependence of bulk diffusion coefficient on $D'\delta$ value measured by curves of the kind displayed in Fig. 3.

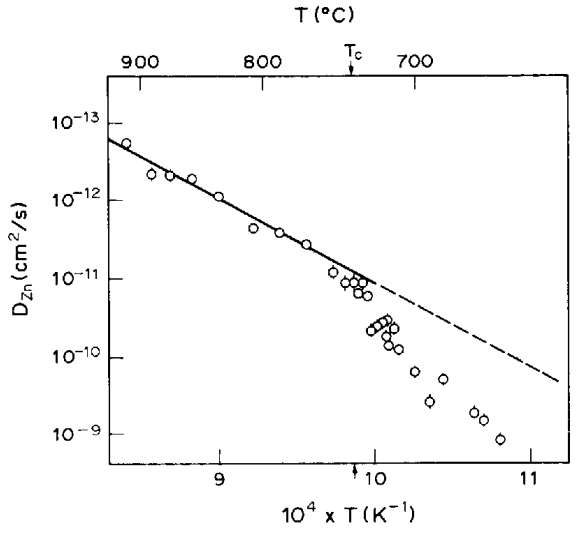

Fig. 5. Thermal dependence of zinc bulk diffusion coefficient in alloy Fe–5 at.% Si along [100] direction (determined by Lyubov's method [34] for o at.% of Zn).

Within the standard assumptions of the Fisher's model [38, 39] we obtain from the equation (1)

$$c = (c_0 - \beta c_0^2/3\pi)\exp(-py) + (\beta c_0^2/3\pi)\exp(-2py) \quad (4)$$

where

$$p = (2\sqrt{D_0}/D'\delta\sqrt{\pi t})^{1/2}.$$

For small y (c is near c_0), usual Fisher's method (2) is valid, but if concentration dependence of bulk diffusion coefficient is taken into account, the equation (2) transforms into

$$D'\delta_{true} = 2y^2\sqrt{D^0/\pi t}\,(1 + 2\beta c_0/3\pi)/[\log(c_B/c_0)^2. \quad (5)$$

The activation energy E and pre-exponential diffusion factor D_0 (for grain boundaries E_b and $D_{0b}\delta$ respectively) were defined by obtained values of bulk and grain-boundary diffusion coefficients for different temperatures using the Arrhenius equation and processing the data by the least-square method.

In our experiments, the diffusion coefficients both above and below Curie point were measured. The matrix transition from paramagnetic into ferromagnetic state is known, although, to affect greatly self- as well as heterodiffusion: in ferromagnetic state the diffusion activation energy is higher than in paramagnetic and below the Curie point lies a transition region between paramagnetic and ferromagnetic Arrhenius laws; in this region the diffusion coefficient falls with temperature dramatically [40–47]. In iron and its alloys the transition interval thickness equals about 100°C [41, 43–46]. This roughly corresponds to the temperature interval in which spontaneous magnetization of iron falls to zero [48, 49]. The activation energy in this temperature interval is very high and rejects traditional interpretation as in ferromagnetic and paramagnetic regions [42, 46]. So in the present work we have determined activation energies and preexponential factors only in paramagnetic region.

3. RESULTS

3.1. The results of bulk and grain boundary diffusion coefficients measurements

The results of measurements of tin and zinc bulk diffusion coefficients are displayed in Tables 1 and 2. In Figs 4 and 5 thermal dependences of bulk diffusion coefficients are plotted in Arrhenius coordinates. These dependences are divided into two regions by Curie point: the paramagnetic above T_c and the critical one below T_c. The Curie point was determined as the point of the highest curve slope in Arrhenius coordinates. The T_c values for the Fe–Si alloy studied are equal, according to our data, to 740 ± 2°C. That value coincides with the T_c value for the Fe–5 at.% Si alloy, obtained by other methods [29]. Tin diffusion coefficient does not depend on concentration, and for zinc the D^0 values determined by Lubov's method for 0% Zn are displayed in Fig. 5

Table 2. The zinc bulk and grain boundary diffusion coefficients in Fe–5 at.% Si alloy

Temperature (°C) 1	Anneal duration (10^4 s) 2	Bulk diffusivity $\times 10^{17}$ m^2/s, 0% Zn 3	Bulk diffusivity $\times 10^{17}$ m^2/s, 5% Zn 4	Grain-boundary diffusion coefficient D′δ 10^{20}m^3/s I 5	II 6
908	1.08	5570	7320	3100 ± 800	
890	0.72	2220	3190	3500 ± 1100	20
875	1.98	2060	2870	2100 ± 500	20
857	2.70	1970	2200	1700 ± 400	30
836	4.68	1080	1200	1000 ± 300	
809	7.56	440	460		
790	22.68	360	480		
772	39.60	270	310	280 ± 50	
753	36.00	120	120	200 ± 40	0.3
745	60.12	87	100		
740	28.08	87	100		
737	48.60	62	72		
734	43.20	81	97	98 ± 11	
731	34.20	57	66	56 ± 8	10
728	30.60	21	26	67 ± 6	
725	28.80	24	34		
721	34.56	27	33		
719	49.32	18	23	45 ± 6	
719	61.20	28	36	40 ± 6	0.1
717	43.56	13	16	16 ± 1	
714	76.50	22	30	31 ± 6	
711	83.52	18	27	26 ± 6	
702	68.40	5.9	7.7		
692	77.76	2.5	2.7	3.7 ± 1.9	0.04
685	90.18	4.9	5.3	1.6 ± 0.8	0.03
667	101.52	1.8	1.9	1.6 ± 0.4	
662	86.40	1.4	1.5	0.7 ± 0.3	
652	293.76	0.8	0.8	0.8 ± 0.2	

and Table 2. The activation enery E_p and pre-exponential factor D_{0p} for bulk diffusion of zinc and tin in paramagnetic region are displayed in Table 3.

Table 2 demonstrates the results of product $D'\delta$ measurements for zinc diffusion along tilt grain boundary 43° [100] (the general boundary). As noted in Section 2, we determined $D'\delta$ for zinc diffusion only at high c_B values, i.e. by gentle regions on Fisher's curves (cf. Fig. 3). Length of such gentle regions was equal to 150 . . . 300 μm which made it possible to determine $D'\delta$ precisely enough. Length of "steep" regions did not exceed 20 μm, so the factor $D'\delta$ value could be determined for them only by the order of magnitude. These data are displayed in the last column of Table 2.

In Fig. 6, the thermal dependence of the factor $D'\delta$ for grain-boundary zinc diffusion is displayed. Qualitatively, it has the same outlook as the thermal dependences of the bulk diffusion coefficients displayed in Figs 4 and 5. The activation energy of zinc grain boundary diffusion E_{bp} and pre-exponential diffusion factor $(D_{0b}\delta)_p$ in paramagnetic region are: $E_{bp} = 192 \pm 2$ kJ/mol; $(D_{0b}\delta)_p = 1.2 \pm 0.2\ 10^{-8}$ m^3/s. The grain-boundary diffusion activation energy value makes 0.79 of bulk diffusion activation energy. Below Curie point, the grainboundary diffusion coefficient falls faster than bulk one.

3.2. The grain boundaries wetting in system (Fe–5 at.% Si)–Sn

Figure 1(b, c) shows the typical concentration profiles of tin on the cross-section specimens of bicrystals 43° [100] Fe–5 at.% Si after diffusional anneal. On the sample surface a layer is situated formed from the iron dissolution in molten tin during the first minutes of anneal. The layer of bulk diffusion lies deeper. In Fig. 1(b) no preferential penetration of tin along grain boundary can be noticed: the isoconcentration lines are parallel to sample surface. This is true for tin concentration profiles in all bicrystal samples annealed at temperatures below 810 . . . 815°C. At higher temperatures the picture changes dramatically: a thin (roughly 1 μm) layer enriched by tin can be seen along grain boundaries

Table 3. The parameters of bulk self- and heterodiffusion by published data and by results of our experiments

Matrix	Diffusant	E (kJ/mol)	$D_0 \times 10^4$ (m^2/s)	Temperature range (°C)	Reference
α-Fe	^{59}Fe	256.7	1.67	809 901	[55]
α-Fe	^{59}Fe	266.3	10	1000–1043	[56]
α-(Fe–7.64% Si)	^{59}Fe	228.2	1.38	900–1100	[41]
α-(Fe–11% Si)	^{59}Fe	212.3	0.63	900–1100	[41]
α-Fe	Zn	264	60	800–910	[45]
α-Fe–5% Si)	Zn (0%)	227 ± 3	5 ± 2	750–908	This work
α-(Fe–5% Si)	Zn (5%)	243 ± 3	32 ± 7	750–908	This work
α-Fe	^{113}Sn	222	2.4	800–910	[65]
α-(Fe–5% Si)	Sn	210 ± 1	0.9 ± 0.1	750–908	This work

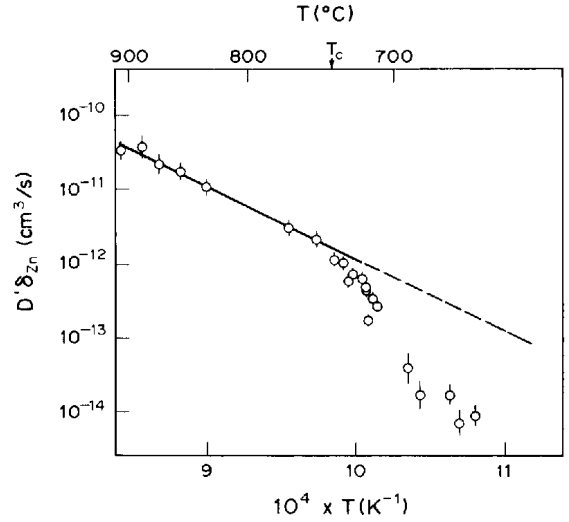

Fig. 6. Thermal dependence of product of grain boundary diffusion coefficient D' and diffusional grain-boundary thickness δ for zinc diffusion by tilt grain boundary [100] 43° in alloy Fe–5 at.% SI.

[cf. Fig. 1(c)]. The tin concentration in this layer reaches or even exceeds the solubility limit of tin in iron-based solution (c_0). The layer thickness is roughly constant regardless of the depth. The depth of penetration of the layer along the grain boundary L makes $10 \ldots 10^2$ μm from the sample surface. It is independent of the anneal temperature and duration. We have only revealed a weak correlation between the depth L and the initial tin layer thickness on the sample surface: the thicker is the layer, the larger is the L value. Here noticeable diffusion of tin along a grain boundary is also absent.

These facts witness that at temperature $T_w = 810 \ldots 815$°C occurs the phase transition of wetting of grain boundary 43° [100] Fe–5 at.% Si by the melt (FeSi)–Sn. Below T_w the contact angle θ at the site of grain boundary intersection with the interface "solid phase-melt" is near to 180°, while above T_w the θ angle is equal to zero (this corresponds

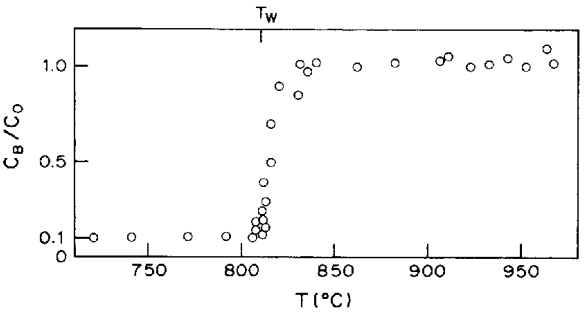

Fig. 7. Thermal dependence of tin concentration c_B in tilt grain boundary 43° [100] in Fe–5 at.% Si alloy. c_0 is the solubility limit of tin in bcc solid solution. The c_B value was measured at such distance from the surface, at which the concentration c in the bulk diffusion layer far from the boundary equals to $0.1c_0$. These positions are marked in Fig. 1(b, c) by black points. At temperature $T_w = 810 \pm 5$°C, a wetting transition occurs. Above this temperature, there exists a thin equilibrium wetting layer on grain boundaries.

to long and thin layer at grain boundaries). We did not measure the contact angle θ in the interval of temperature around T_w (where θ changes from 180° to zero) because in our case this angle was not equilibrium. It was so, because the initial composition of bicrystal differs from the equilibrium c_0 corresponding to the solidus line (θ angle must change during anneal on account of changes in composition of the solid phase surface layers because of diffusion). So we have plotted the thermal dependence of tin concentration on grain boundary c_B in the points lying at distance $y_{0.1}$ from the sample surface (Fig. 7). At distance $y_{0.1}$ from the surface, the tin concentration in the layer of bulk diffusion far from the grain boundary makes up $c(y_{0.1}) = 0.1c_0$ [black points in Fig. 1(b, c). At $T < 810$°C the concentration on the boundary $c_B = 0.1c_0$, while at $T > 810$°C it makes $c_B \approx (0.9\text{–}1.2)c_0$. Between 810° and 820°C the c_B value increases gradually from $0.1c_0$ up to $0.9c_0$. Therefore, the wetting transition point (wetting of tilt grain boundaries 43° [100] Fe–5 at.% Si by the melt (FeSi)–Sn) $T_w = 810 \pm 5$°C.

We should stress once more that above the T_w point at which the wetting transition occurs, we have not revealed any changes of grain boundaries properties below the wetting layer. We have observed such changes in boundaries properties below the wetting layer in course of zinc penetration along the grain boundaries.

3.3. Wetting and grain boundary phase transition in system (Fe–5 at.% Si)–Zn

In Fig. 1(d), the zinc concentration distribution after annealing at 908°C for 3 h is displayed. Some features of this distribution resemble those of tin concentration distribution in Fig. 1(c). We see again the layer of bulk diffusion, the layer of high zinc concentration along the grain boundary formed at the initial stage of diffusional anneal, and also the unperturbed layer of bulk diffusion in the vicinity of high-concentration layer. There is also a substantial difference: a region of high diffusivity can be clearly seen deeper than the grain boundary wetting layer [its beginning and end are marked by arrows in Fig. 1(d)]. That region can be identified with the gentle region on Fisher's dependences of the concentration on grain boundary c_B upon depth y (cf. Fig. 3). The value of the $D'\delta$ product at that region is very large: it is roughly by 2 orders of magnitude higher than characteristic value of $D'\delta$ for grain boundary self- and hetero-diffusion in b.c.c.-iron [50–53]. At the steep region the $D'\delta$ value near to usual is observed [50–53].

We have already indicated that the length of the grain boundary wetting layer (where the tin or zinc concentration is higher than bulk solubility limit) does not depend on the anneal temperature and duration. This is indicative of the non-diffusional mechanism of penetration of substance along the grain boundaries. Although below the wetting layer

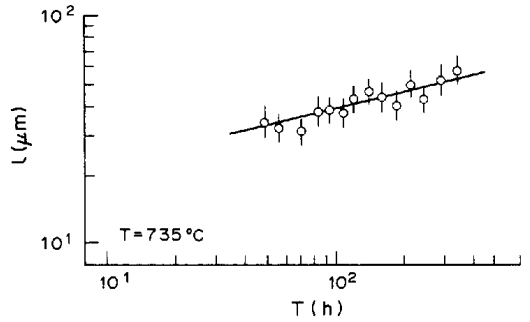

Fig. 8. The dependence of distance l at which the logarithm of grain boundary zinc concentration decreases from -1 to -1.1 on the anneal duration at constant temperature 735°C. It can be seen by the slope of the line that the law $l \simeq t^{1/4}$ is valid.

the substance also does rapidly penetrate along the boundaries, that is the diffusional process. If a substance diffuses rapidly along the layer of thickness δ with the simultaneous "drawing off" into bulk (with the bulk diffusion coefficient D and $D' \gg D$), then the penetration distance L_B of a substance along a grain boundary is proportional to $t^{1/4}$. In Fig. 8, the dependence of penetration distance of zinc along the grain boundary 43° [100] at the 735°C on the annealing time is displayed. L_B was determined as a distance at which $\log c_B$ decreases from -1 to -1.1. The annealing time varied from 48 up to 331.5 h (totally 14 values). The slope of the line in Fig. 8 is indeed equal to 1/4. It can also be seen in Fig. 9 that the c_{Bt} value is independent of annealing time. This attests that the c_{Bt} concentration is equilibrium.

In our opinion, the data reported indicate that at concentration c_{Bt}, a phase transition accompanied by formation of thin wetting layers occurs on grain boundaries. This transition was not observed in our experiments with tin. When the line of such transition is crossed, the boundary thickness δ should increase abruptly. If the grain boundary diffusivities D' above and below c_{Bt} can be assumed equal to one another, then the thickness of the wetting layer on grain boundary can be estimated by ratio of values $D'\delta$ above and below c_{Bt}. This ratio makes up roughly 10^2.

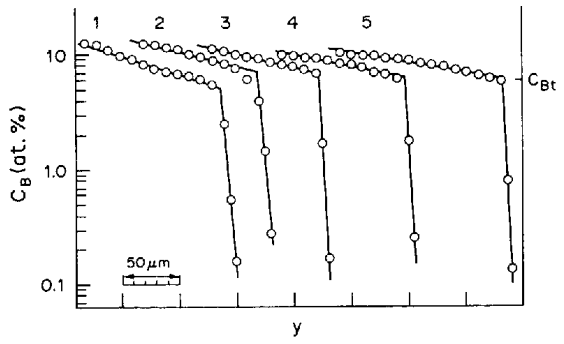

Fig. 9. The dependence of zinc concentration on the boundary c_B on depth y for constant temperature 735°C and various time of anneal t. It can be seen that c_{Bt} does not depend on t. 1—48 h; 2—80 h; 3—118.8 h; 4—281 h; 5—331.5 h.

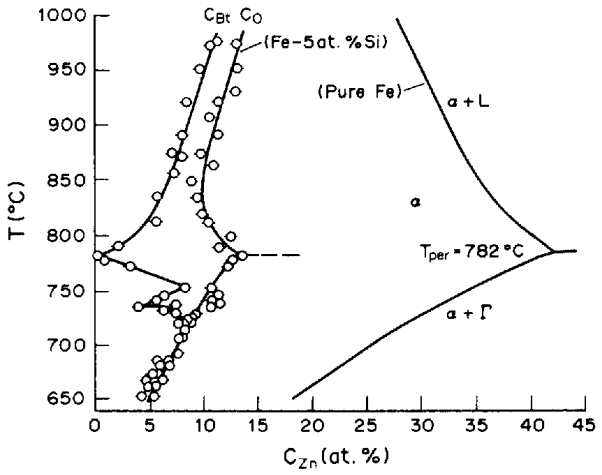

Fig. 10. The thermal dependences of c_{Bt} and c_0. The zinc concentration is plotted on x-axis. The line of solubility limit of zinc in pure iron is also displayed (solidus and solvus) [29].

The temperature dependence of c_{Bt} is displayed in Fig. 10. In this figure, the line of solubility limit of zinc in the Fe–5 at.% Si alloy according to our data and that of zinc in pure iron according to [29] are displayed. The maximum of solubility is observed at the peritectics temperature. Our data on the solubility limit are in agreement with the results obtained by traditional methods of analysis of Fe–Si–Zn ternary diagram: even a small addition of silicon drastically decreases the solubility limit of zinc in Fe [54]. The distinct appearance of the wetting transition line on the iron–zinc phase diagram can be explained, in our opinion, by the fact that the solubility limit line c_0 in this system goes very close to the metastable line of the solid solution decomposition obtained by thermodynamic calculations [30]. The $c_{Bt}(T)$ line has rather complicated form. Above the Curie point the c_{Bt} concentration value is the lower, the greater is the bulk solubility limit c_0. In the vicinity of the Curie point this correlation is distorted: the line has a protuberance faced to the lower zinc concentrations.

4. DISCUSSION

4.1. Diffusion in paramagnetic region

Silicon is known to diminish the self-diffusion activation energy of iron if Fe–Si alloys (cf. Table 3). It is easy to understand this fact because silicon decreases also the melting point of iron, and correlation between the self-diffusion activation energy and melting temperature is widely known. So the values of zinc and tin diffusion activation energies for the bulk of Fe–5 at.% Si alloy obtained by us are smaller than standard values for tin and zinc bulk diffusion in pure iron.

The activation energy of tin diffusion in pure iron is by 30 . . . 40 kJ/mol smaller than self-diffusion activation energy of iron (cf. Table 3). The tin diffusion activation energy value obtained by us is also by roughly 34 kJ/mol smaller than E for iron self-

Table 4. The critical indices d for magnetic part of bulk and grain boundary self- and heterodiffusion activation free energy ΔG_m obtained by processing of published data and results of our measurements

Material	Diffusant	d	Reference
α-Fe	^{59}Fe	0.9 ± 0.2	[43, 44]
α-Fe	Zn	0.8 ± 0.1	[45]
α-Fe	Co	0.8 ± 0.1	[46]
α-Fe–7.64 at.% Si)	^{59}Fe	0.93 ± 0.05	[14]
α-(Fe–5 at.% Si)	Sn	0.7 ± 0.1	This work
α-(Fe–5 at.% Si)	Zn (0%)	0.8 ± 0.3	This work
α-(Fe–5 at.% Si)	Zn (5%)	1.0 ± 0.3	This work
α-(Fe–5 at.% Si)	Zn (by grain boundary)	1.2 ± 0.3	This work

diffusion in Fe–5 at.% Si alloy (if data of [41, 55, 56] are interpolated to Fe–5 at.% Si alloy; $E_{Fe} = 243$ kJ/mol). The zinc diffusion activation energy in the bulk of paramagnetic α-iron practically coincides with iron self-diffusion activation energy (cf. Table 3). The E values for zinc diffusion determined by us are also nearly the same as that for iron self-diffusion in Fe–5 at.% Si alloy. The Lasarus' model [57] predicts the changes of vacancy formation and migration energy in diluted solution to be proportional to the difference between valencies of solute and solvent. The obtained results mean that valency states of tin and zinc in iron and Fe–5 at.% Si alloy practically do not differ; zinc and iron valencies coincide, and tin valency in the solution is less than iron valency. Really, tin is in the group IV of the periodic table, and iron in most cases has valency 2 or 3. Therefore, our data on activation energies and pre-exponential factors of the bulk diffusion in paramagnetic region are, on the whole, in reasonable agreement with data given in literature, and do not contradict to the hypothesis of vacancy mechanism of diffusion in α-iron.

The $D'\delta$ values for zinc grain boundary diffusion in the whole studied paramagnetic region belong to the same Arrhenius curve (cf. Fig. 7). This must mean that zinc diffusion mechanism remains unchanged above Curie point. The grain boundary diffusion activation energy value makes up 0.8 of that of the bulk diffusion. Usually the activation energy of grain boundary diffusion of isotopes in iron and its alloys makes up 0.4 . . . 0.6 of activation energy of bulk diffusion [50–53]. Only in investigations [58, 59] this ratio was found to grow from 0.6 up to 0.85 with increase of sulphur concentration. The nearness of E for grain boundary to bulk value means that the region of fast grain boundary diffusion ($c_B > c_{Bt}$), for which the $D'\delta$ values have been determined, occupies the intermediate position between usual grain boundary and bulk and, probably, is impurities enriched.

4.2. Diffusion in critical region below Curie point

The existing published data and results of present work witness that diffusion in iron goes by vacancy mechanism. Then thermal dependence of diffusion coefficient must have the form

$$D = gfa^2 \nu \exp(-G/RT) \tag{6}$$

here g is the geometric factor, f is the correlation factor, a is the lattice parameter, ν is the frequency of thermal oscillations of atoms, G is the activation free energy. We shall assume the values of f and ν to remain unchanged after transition through Curie point. We divide the activation free energy into paramagnetic (p subscript) and magnetic (m subscript) components

$$G = G_p + G_m. \tag{7}$$

It is commonly recognized that the critical behavior of the diffusion coefficient below the Curie point may be explained assuming

$$G_m = \alpha M^2 \tag{8}$$

where M is spontaneous magnetization. Although in advanced theories of magnetic effect more complex expressions for G_m were derived [41, 46], for our rough data formula (8) is a good approximation. The α value depends on parameters of interatomic interactions. So we can, using our experimental data, determine α values for the bulk and grain boundary. But the α value is of little interest for us. What we want to know is the information about the layer of rapid grain boundary diffusion. For that purpose a critical indices formalism, widely used in the theory of phase transition and critical phenomena is very useful. In the vicinity of the second-order phase transitions (particularly, ferromagnetic–paramagnetic transition) the derivatives of free energy (for example, specific heat, susceptibility) and connected variables depend on temperature by power law, for example.

$$\chi \sim |T - T_C/T_C|^{-\gamma}. \tag{9}$$

Here γ is the so-called critical index for susceptibility χ. Critical indices are important parameters of a system near phase transition. In order to characterize behaviour of the diffusion coefficients in critical region below the Curie point, we shall use the critical index d for magnetic contribution G_m into the activation free energy G. Using (6) and (7) one can write

$$G_m = RT(\log D_{extr} - \log D) \tag{10}$$

where $D_{extr} = gfa^2 \nu \exp(-G_p/RT)$. The critical exponent d for magnetic part of free energy can be determined by plotting $\Delta G_m/R$ dependence upon $|T - T_c|/T_c$ in log–log coordinates. Here

$$\Delta G_m = G_m(T) - G_m(T_c). \tag{11}$$

It is clear from the equation (8) that the d value must be twice as large as the critical index β for the

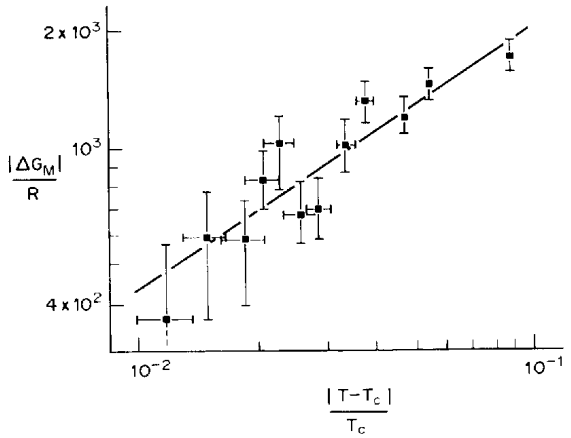

Fig. 11. The dependence of magnetic part of activation free energy $\Delta G_m/R$ upon $|T - T_c|/T_c$ plotted in scaling coordinates for bulk diffusion of tin in Fe–5 at.% Si alloy in critical region below Curie point T_c.

magnetization M. In Fig. 14, thermal dependences of ΔF_m obtained from Refs [41, 43–46] for diffusion in iron and its alloys are plotted in $(\Delta G_m/R) - (|T - T_c|/T_c)$ coordinates. In Table 4 are displayed the values of critical index d for magnetic part of the free energy ΔG_m defined by these plots (Fig. 14) along with d values for the present work (Figs 11–13). It can be seen that critical index d values for bulk diffusion both by our and references data are equal to about 0.8–0.9. Indeed, these values are approximately equal to 2β values, where $2\beta = 0.77$ for pure iron and $2\beta = 0.86$ for Fe – 5.86 at.% Si alloy [60].

At the same time, critical index for zinc grain boundary diffusion turned out to be significantly higher than bulk value (cf. Table 4). How can it be explained? First we shall argue, which value must have the critical index for "usual" grain boundary whose thickness is two or three lattice parameters [1]. If we assume that the role of the grain boundary is to reduce exchange interactions only for electrons

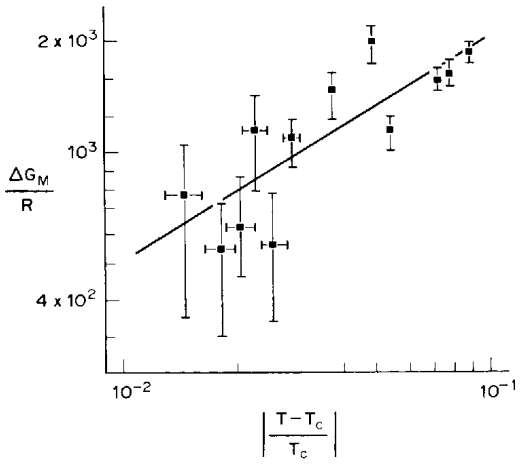

Fig. 12. The dependence of magnetic part of activation free energy $\Delta G_m/R$ upon $|T - T_c|/T_c$ plotted in scaling coordinates for bulk diffusion of zinc in Fe–5 at.% Si alloy in critical region below Curie point T_c.

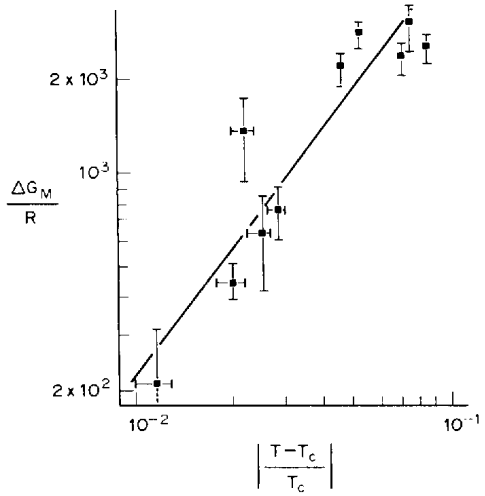

Fig. 13. The dependence of magnetic part of activation free energy $\Delta G_m/R$ upon $|T - T_c|/T_c$ plotted in scaling coordinates for grain boundary zinc diffusion in Fe–5 at.% Si alloy in critical region below Curie point T_c.

near the boundary then this problem is equivalent to that of determining of surface magnetization of ferromagnetic crystal. In works [61, 62] the surface magnetization was shown to change with temperature near T_c by power law, and the corresponding critical exponent β_s exceeds the bulk value by a factor of 2. The critical index for two-dimensional diffusion in

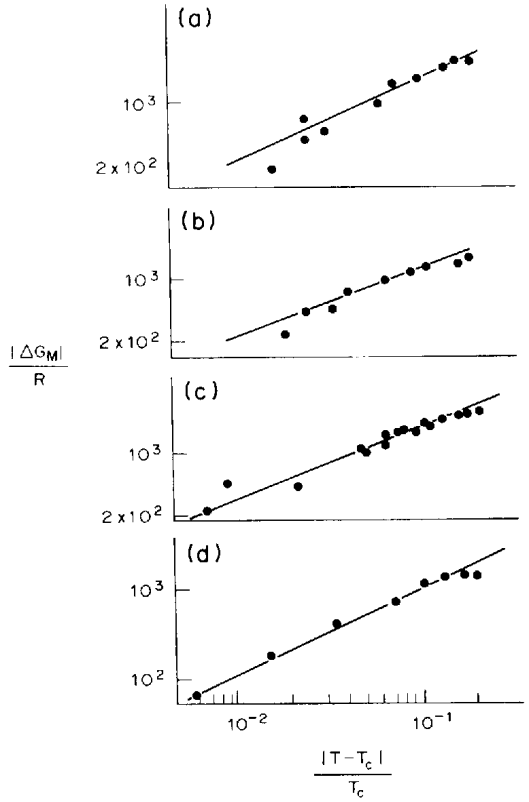

Fig. 14. The dependence of magnetic part of activation free energy $\Delta G_m/R$ upon $|T - T_c|/T_c$ plotted in scaling coordinates for bulk diffusion in iron by published data: A—self-diffusion in α-Fe [43, 44]; B—zinc diffusion in α-Fe [45]; C—cobalt diffusion in α-Fe [46]; D—iron self-diffusion in Fe-7.64 at.% Si alloy [41].

such grain boundary must be, according to these considerations, $d \approx 1.6$.

Therefore, the critical index for the "fast" grain boundary diffusion below Curie point lies between the measured value for three-dimensional system and hypothetic value for "thin" grain boundary. Here we see a definite similarity to the behaviour of zinc grain boundary activation energy above Curie point, in paramagnetic region (cf. Section 4.1): there E for diffusion along the high-concentrational layer is also between E value for bulk diffusion and E values for typically grain boundary diffusion when diffusional thickness of grain boundary δ is near to the lattice parameter. Unfortunately, we can not compare the critical exponents for "fast" and "usual" grain boundary diffusion, because detailed data on grain boundary diffusion in critical region below Curie point are absent.

Consequently, results of our study of zinc grain boundary diffusion both below and above T_c indicate that the layer of "rapid" grain boundary diffusion is too thick to be two-dimensional. We shall now try to understand the nature of the observed grain boundary phase transition and to explain the peculiarities of the c_{Bt} line.

4.3. The grain boundary phase transition in system (Fe–5% Si)–Zn

When $c_B = c_{Bt}$, the value of the product of the grain boundary diffusion coefficient and the boundary thickness $D'\delta$ decreases abruptly by two orders of magnitude. We suppose a phase transition accompanied by grain boundary "thickening" to occur at $c_B = c_{Bt}$. What may be the nature of this transition?

It is known [16] that all the miscellany of the wetting phenomena may be obtained from an analysis of the wetting layer free energy Ω_s:

$$\Omega_s = 2\sigma_{cf} + l\Delta g + V(l). \tag{12}$$

Here, σ_{cf} is the surface tension of the "crystal-wetting phase" interphase, l is the wetting layer thickness, Δg is the excess free energy of the wetting phase. The latter term describes the interaction of the "crystal-wetting phase" interphases. The situation in which the wetting layer thickness goes into infinity ($l \Rightarrow \infty$) when the line of phase co-existence is approached ($\Delta g \Rightarrow 0$), is called the complete wetting. Because the equilibrium thickness of the wetting layer is determined by minimization of (12) with regard to l, so the complete wetting can be observed only in case, when two conditions are satisfied

$$\text{(I)}\quad 2\sigma_{cf} < \sigma_{gb}$$

where σ_{gb} is the grain boundary surface tension.

$$\text{(II)}\quad V(l) \text{ must have the global minimum in point } l = \infty.$$

In other words, the interfaces "crystal-wetting phase" must repel one another. We assume the V depends on l by power law

$$V(l) = W/l^n. \tag{13}$$

If Δg value is large (far from phase co-existing line), then $\Omega_s(l_0) > \sigma_{gb}$ (here l_0 is the l value at which $\Omega_s(l)$ function has a minimum, and the wetting layer on the boundary is unprofitable (the boundary is "clean" [Fig. 15(A)].

When Δg is such that $\Omega_s(l_0) = \sigma_{gb}$, then the boundary transforms into a thin layer of a wetting phase of thickness l_0 [Fig. 15(*b*)]. This is so-called premelting transition on grain boundary if the wetting phase is liquid. When Δg decreases, the l_0 value grows and becoms infinity for $\Delta g = 0$ [Fig. 15(c, d)].

Consequently, when zinc concentration near grain boundary reaches c_{Bt}, then on the boundary a premelting transition occurs—the boundary is replaced by a thin layer of a phase enriched by zinc. The region of accelerated diffusion is observed at all studied temperatures: both above and below the peritectics temperature (cf. Fig. 10). Our data do not allow to distinguish the true premelting from the transition in which the solid phase is involved. Both transitions are described by the same thermodynamic scheme (Fig. 15). So further we shall call our transition just the premelting transition. Consider which corollaries this assumption has.

4.4. Correlation between $c_{Bt}(T)$ and $c_0(T)$

At c_B equal to the bulk solubility limit c_0 (solvus or solidus) we have $\Delta g = 0$. For small deviations from

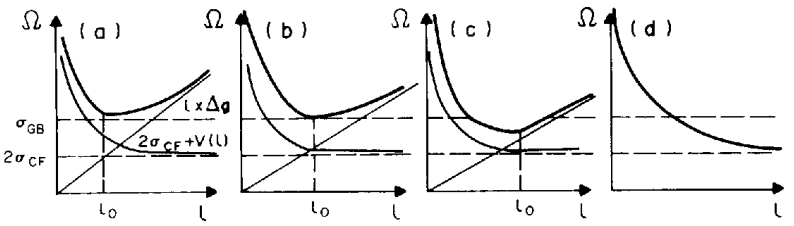

Fig. 15. The dependences of extra free energy of wetting layer Ω on the layer thickness l. σ_{cf}-the surface tension of the interphase "crystal-wetting phase"; σ_{gb}-the grain boundary surface tension (marked by dashed horizontal lines). In (a c) the hyperbola $V(l)$ and the straight line $l\Delta g$ are shown. Along with $2\sigma_{cf}$ these yeld $\Omega(l)$. (a) Wetting layer on a boundary is not profitable; (b) Ω tangents σ_{gb}, and on a boundary a thin layer of wetting phase of thickness l_0, appears (the premelting transition); (c) in the course of further decrease of Δg, the layer thickness grows; (d) at $\Delta g = 0$ the layer thickness l_0 goes to infinity (complete wetting).

c_0 we shall expand Δg into a series in terms of c_0–c_B. Truncation by the first term of this expansion yields

$$g = b(c_0 - c_B) \tag{14}$$

the $\Omega_s(l)$ function determined by use of equations (12), (13) and (14), has a minimum at

$$l_0 = [b(c_0 - c_B)/nW]^{-1}/(n+1). \quad \Omega_s(l_0) = \Omega_0 = 2\sigma_{cf} + (nW)^{1/n+1}\,[b(c_0 - c_B)^{n/n+1}(1 + W^{-1}).$$

When the condition $\Omega_0 = \sigma_{gb}$ is satisfied, then the premelting transition occurs: the grain boundary is replaced by a layer of a phase enriched by zinc. From this condition we obtain

$$c_{bt} = c_0 \frac{(\sigma_{gb} - 2\sigma_{cf})^{(n+1)/n}}{b(Wn)^{1/n}(1 + W^{-1})^{(n+1)/n}}. \tag{15}$$

The equation (15) connects the bulk solubility limit with the concentration at which the premelting transition occurs at the boundary. But the surface tensions σ_{gb} and σ_{cf} also depend on concentration, so it is not so easy to compare (15) with the experimental data. Luckily, in system Fe–Zn the solubility limit line (solvus) is near to the metastable curve of solid solution decomposition [29]. This means that the σ_{cf} value falls dramatically when the peritectics transformation point is approached. This, according to formula (15) must lead to c_{Bt} decrease, which is actually observed in the experiment.

4.5. The ferromagnetism influence on the wettability of the grain boundaries

Consider a tilt grain boundary [100] in a thin ferromagnetic plate. We assume that the grain boundary is wetted by a thin layer of non-ferromagnetic phase of thickness l. We assume that the mean domain size d is independent of l (this corresponds to pinning of domain walls by lattice defects). The interaction of magnetic fields which appear in the vicinity of interphase "crystal-wetting phase" will lead to an extra term in (12) which we denote $V_m(l)$. This term corresponds to attraction of the two mentioned interfaces (remember that if magnet is cut in two, the fragments attract one another). Qualitatively $V_m(l)$ function may be represented as follows: at a low l values $V_m(l)$ contains the magnetostatic energy of the magnetic field inside the paramagnetic wetting film. When $l \ll d$ one can neglect the curvative of the lines of magnetic force and $V_m(l) = 2\pi M^2 l \sin^2(\phi/2)$, where ϕ is misorientation angle. The larger the wetting film thickness, the higher is the magnetostatic energy inside the film, and at some l_{crit} the flux-closure domains formation is favorable. In such a domain the magnetization direction is parallel to one of the easy magnetization axes lying parallel to the wetting film. In our case the axes [100] are common for two crystals. Then the magnetostriction energy would be taken into account in $V_m(l)$ calculation. It may be estimated by the magnetic anisotropy energy: $V_m(l) = \beta M^2 d$. The l_{crit} value may be obtained from the condition $2\pi M^2 l \sin^2(\phi/2) = \beta M^2 d$. Assuming $\beta \approx 3 \cdot 10^{-4}$ [63], $d \approx 10^{-3}$ cm we obtain $l_{crit} = 2 \cdot 10^{-7}$ cm. Therefore the flux-closure domains will exist around the wetting film practically at all l values. Should the direction of magnetization be exactly parallel to the boundary plane, the magnetic field would not exist inside the wetting film, and the ferromagnetism would not have any influence on the wetting transition. But in the bicrystal of Fe–5 at.% Si alloy studied the [100] axes common for both crystals are misoriented by the angle $\Delta\phi \approx 3°$ with respect to each other. Consequently, the magnetization in flux-closure domains would have a component $M_\perp = M \sin\Delta\phi$ perpendicular to the wetting film plane. In this case magnetic field would be inside the wetting film. Then the part of $V_m(l)$ which depends on l may be written as follows

$$V_m(l) \approx 2\pi M_\perp^2 l = 2\pi M^2 l \sin^2(\Delta\phi), \qquad l_{crit} < l \ll d. \tag{16}$$

The function $V(l)$ from (13) may be estimated by the monotonic part of the electron contribution to the free energy of a thin metallic film [64]

$$V(l) = N_s E_F \frac{\chi}{(3\pi^2)^{2/3}} \frac{a}{l} \approx 10^3 \chi \frac{a}{l}\ \text{erg/cm}^2 \tag{17}$$

where E_F is the Fermi energy of the film material, χ is a constant depending on the material properties, χ can change from 0 to 2; N_s is the number of atoms in 1 cm^2 of monolayer. In order to estimate $V(l)$ function we have taken numerical values for the typical metal: $E_F \approx 10^{-11}$ erg and $N_s \approx 10^{15}$. Then for total potential $V_t(l)$ of "crystal-wetting phase" interfaces interaction taking into account equations (16) and (17) we will have

$$V_t(l) = 2\pi M^2 l \sin^2(\Delta\phi) + 0.1\chi N_s E_F (a/l). \tag{18}$$

This function has a minimum at

$$l_m = \frac{1}{M \sin\Delta\phi} \frac{\sqrt{0.1\chi E_F N_s a}}{2\pi}$$

its value at this point is

$$E_m = 2M \sin\Delta\phi \sqrt{0.2\chi\pi N_s E_F a}.$$

When $l \Rightarrow \infty$ then $V(l) \Rightarrow V_m^\infty(l) \approx 1.7 M^2 d \sin^2(\Delta\phi)$. When $E_m < V_m^\infty(l)$ the condition of complete wetting is not realised: $V(l)$ function hasn't global minimum at $l \Rightarrow \infty$. From this condition one can obtain

$$M > \frac{2\sqrt{0.2\chi\pi N_s E_F a}}{1.7 d \sin(\Delta\phi)} \approx 400\ \text{Gs, when } \chi \approx 2.$$

It should be noted that the ferromagnet has a magnetization $\simeq 400$ Gs at temperatures 10–20°C below the Curie point. Therefore the magnetic ordering suppresses effectively the grain boundary wetting. Indeed, at temperatures $\simeq 720$°C (which is by 20°C lower than the Curie point in alloy Fe–5 at.% Si) the line of grain boundary phase transition practically meets the solubility limit line (cf. Fig. 10). Below this

temperature, the gentle regions on Fisher's dependences are characterized by poor reproducibility, so the premelting line is marked for this temperature by dotted line. Consequently we may say that at 720°C premelting and wetting are suppressed by ferromagnetism. To tell the truth, we should note that we observe the wetting layer down to the lowest values of temperature (650°C). This may be connected with the fact that contact of premelting line and solvus line $c_0(T)$ is tangential and random fluctuations of the composition lead to a substantial shift of wetting transition point.

Acknowledgements—The authors wish to thank Professors D. E. Khmelnitsky and G. V. Uimin for useful discussion, and Professor S. Dietrich for given opportunity to read his review "Wetting Phenomena" before publication.

REFERENCES

1. T. J. Tan, S. L. Sass and R. W. Balluffi, *Phil. Mag.* **31,** 575 (1975).
2. M. Schick, *Progr. Surf. Sci.* **11,** 245 (1981).
3. M. Hashimoto, Y. Ishida, R. Yamamoto and M. Doyama, *Scripta metall.* **16,** 267 (1982).
4. M. Hashimoto, Y. Ishida, R. Yamamoto and M. Doyama, *Acta metall.* **32,** 1 (1984).
5. V. Vitek, A. P. Sutton, G. J. Wang and D. Schwartz, *Scripta metall.* **17,** 183 (1983).
6. R. Kikuchi and J. W. Cahn, *Phys. Rev. B* **21,** 1983 (1980).
7. R. Kikuchi and J. W. Cahn, *Phys. Rev. B* **36,** 418 (1987).
8. C. Rottman, *Phil. Mag. A* **55,** 499 (1987).
9. K. E. Sickafus and S. L. Sass, *Acta metall.* **35,** 69 (1987).
10. A Greenberg, Y. Komem and C. L. Bauer, *Scripta metall.* **17,** 405 (1983).
11. L. S. Shvindlerman and B. B. Straumal, *Acta metall.* **33,** 1735 (1985).
12. E. L. Maximova, L. S. Shvindlerman and B. B. Straumal. *Acta metall* **36,** 1573 (1988).
13. E. L. Maximova, E. I. Rabkin, L. S. Shvindlerman and B. B. Straumal, *Acta metall.* **37,** 1995 (1989).
14. E. I. Rabkin, L. S. Shvindlerman and B. B. Straumal, *J. less-common Metals* **159,** 43 (1990).
15. P. G. De Gennes, *Rev. Mod. Phys.* **57,** 827 (1985).
16. S. Dietrich, in *Phase Transitions and Critical Phenomena* (edited by C. Domb and J. Lebowitz, pp. 1–218, vol. 12. Academic Press, New York (1988).
17. A. Passerone, N. Eustathopoulos and P. Desré, *J. less-common Metals* **52,** 37 (1977).
18. A. Passerone and R. Sangiorgi, *Acta metall.* **33,** 771 (1985).
19. K. K. Ikeuye and C. S. Smith, *Trans, Am. Inst. Min. Engrs* **185,** 762 (1949).
20. N. Eustathopoulos, L. Coudurier, J. C. Joud and P. Desré, *Jl Cryst Growth* **33,** 105 (1976).
21. J. H. Rogerson and J. C. Borland, *Trans. Am. Inst. Min. Engrs* **227,** 2 (1963).
22. A. Passerone, R. Sangiori and N. Eustathopoulos, *Scripta metall.* **16,** 547 (1982).
23. C. Rottman, *J. Physique* **C5,** C313 (1988).
24. T. Nguen, P. S. Ho, T. Kwok C. Nitta and S. Yip, *Scripta metall.* **19,** 993 (1985).
25. G. Cicotti, M. Guillopé and V. Pontikis, *Phys. Rev. B.* **27,** 5576 (1983).
26. T. Nguen, P. S. Ho, T. Kwok, C. Nitta and S. Yip, *Phys. Rev. Lett.* **57,** 1919 (1986).
27. J. Q. Broughton and G. H. Gilmer, *Phys. Rev. Lett.* **56,** 2693 (1986).
28. R. Hultgren *Selected Values of the Thermodynamics Properties of Binary Alloys.* Am. Soc. Metals, Metals Park, Ohio (1973).
29. O. Kubaschewski *Iron–Binary Phase Diagrams.* Springer Berlin, Stahleisen, Düsseldorf (1982).
30. T. Nishizawa, M. Hasebe and M. Ko, *Acta metall.* **27,** 817 (1979).
31. J. W. Cahn, *J. chem. Phys.* **66,** 3667 (1977).
32. S. J. B. Reed, *Electron Microprobe Analysis.* Cambridge Univ. Press (1975).
33. J. P. Stark, *Solid State Diffusion.* Wiley, New York (1976).
34. B. Ja. Liubov, *Diffusional Processes in Inhomogeneous Solids.* Nauka, Moscow (1981). (In Russian.)
35. I. B. Borovski, K. P. Gurov, I. D. Marchukova and Ju. E. Ugaste, *Interdiffusion Processes in Alloys.* Nauka, Moscow (1973). (In Russian.)
36. R. T. P. Whipple, *Phil. Mag.* **45,** 1225 (1954).
37. A. D. Le Claire, *Phil. Mag.* **42,** 74 (1951).
38. J. C. Fisher, *J. Appl. Phys.* **22,** 74 (1951).
39. B. S. Bokstein, Ch. V. Kopetzki and L. S. Shvindlerman, *Thermodynamical and Kinetical Properties of Grain Boundaries in Metals.* Metallurgia, Moscow (1986).
40. L. Ruch, D. R. Sain, H. L. Yeh and L. A. Girifalko, *J. Phys. Chem. Solids* **37,** 649 (1976).
41. H. V. Mirani, R. Harthoorn, T. J. Zoorendonk, S. J. Helmenhorst and G. de Vries, *Physica status solidi* (a) **29,** 115 (1975).
42. J. Kučera, B. Million and J. Razichová, *Physica status solidi* (a) **96,** 177 (1986).
43. G. Hettich, H. Mehrer and K. Maier, *Scripta metall.* **11,** 795 (1977).
44. R. J. Borg and D. J. F. Lai, *Acta metall.* **11,** 861 (1963).
45. I. Richter and M. Feller-Kniepmeier, *Physica status solidi* (a) **68,** 289 (1981).
46. J. Kučera, B. Kozak and H. Mehrer, *Physica status solidi* (a) **81,** 497 (1984).
47. K.-I. Hirano, R. P. Agarvala and B. L. Averbach, *J. appl. Phys.* **33,** 3049 (1962).
48. R. S. Preston, S. S. Hanna and J. Heberle, *Phys. Rev.* **128,** 2207 (1962).
49. H. H. Potter, *Proc. R. Soc.* **146,** 362 (1934).
50. D. W. James and G. M. Leak, *Phil. Mag.* **12,** 491 (1965).
51. C. Leymonic and R. Lacombe, *mem. scient Revue Metall.* **57,** 285 (1960).
52. H. Hänsel, L. S. Stratmann, H. Keller and H. J. Grabke, *Acta metall.* **33,** 659 (1985).
53. J. Geise and C. Herzig, *Z. Metallk.* **70,** 622 (1985).
54. W. Köster and T. Gödecke, *Z. Metallk.* **59,** 605 (1968).
55. V. Irmer and M. Feller-Kniepmeier, *Phil. Mag.* **25,** 1345 (1972).
56. L. De Schepper, G. Knuyt and L. M. Stals, *J. Phys. Chem. Solids* **44,** 171 (1983).
57. D. Lazarus, *Solid St. Phys.* **10,** 71 (1960).
58. D. Threheux, *Scripta metall.* **17,** 933 (1983).
59. D. Treheux, *Acta metall.* **30,** 563 (1982).
60. J. L. Routbort, C. N. Reid, E. S. Fisher and D. J. Dever, *Acta metall.* **19,** 1307 (1971).
61. D. L. Mills, *Phys. Rev.* **B3,** 3887 (1971).
62. K. Binder and P. C. Hohenberg, *Phys. Rev.* **B9,** 2194 (1974).
63. I. A. Privorotzky, *Uspehi Fiz. Nauk.* **108,** 43 (1972). (In Russian.)
64. B. V. Deryagin, N. V. Churaev and V. M. Muller, *Surface Forces.* Nauka, Moscow (1985). (In Russian.)
65. D. Treheux, D. Marchive, J. Delagrange and P. Guiraldenq, *C.r. Acad. Sci.* **C274,** 1260 (1972).